SIAM J. Appl. Math.
Vol. 68, No. 5, pp. 1439–1463


# ASYMMETRIC CHANNEL DIVIDER IN STOKES FLOW*

I. DAVID ABRAHAMS†, ANTHONY M. J. DAVIS‡, AND STEFAN G. LLEWELLYN SMITH‡

**Abstract.** This article examines the classic problem of Stokes flow into a divided channel with, in contrast to previous literature, the divider barrier asymmetrically placed with respect to the moving, parallel channel walls. The boundary value problem is reduced to a Wiener–Hopf equation that is of matrix form and of a class for which no exact solution is known. An explicit approximate solution, in general accurate to any specified degree, is obtained by a recent method which employs Padé approximants. Numerical results exhibit the flows due to moving walls or various combinations of downstream pressure gradients.

**Key words.** Stokes flow, channel flow, Wiener–Hopf technique, matrix Wiener–Hopf equations, Padé approximants

**AMS subject classification.** 78A45

**DOI.** 10.1137/070703211

## 1. Introduction.

A classic problem in two-dimensional creeping flow, having an analogy in plane elastostatics, is the disturbance created by the presence of a semi-infinite barrier in a channel flow (see Figure 1.1) driven by a pressure gradient and or shearing. The "parallel lines" geometry suggests the use of the Wiener–Hopf technique; however, the advantage of the constricting walls in creating unidirectional flows both upstream and downstream is offset by the appearance, in general, of a matrix Wiener–Hopf system. The exception is the case of symmetric geometry which yields Wiener–Hopf equations of standard (scalar) type [1], since then the flow components that are even and odd with respect to the centerline can be considered separately. Despite this simplification, the even problem (no flow across the line of the barrier), which is the case of greater interest, requires an intricate factorization constructed and used by Buchwald and Doran [2] and Foote and Buchwald [3]. An erroneous attempt was presented earlier by Graebel [4] with the aim of achieving better accuracy than the approximate, yet still complicated, solutions given by Koiter [5]. Richardson [6] neglected an important feature of the factorization in [2]. Jensen and Halpern [7] verified the calculations of Buchwald and coworkers in using their solution to examine the role of the stress singularity at the edge of surfactant between thin fluid layers. Without a general procedure for solving matrix Wiener–Hopf problems (see further discussion on this point is section 3.1), an alternative strategy for the biharmonic equation is to employ complex variable techniques, facilitated by the removal of one wall (that is, the receding of one channel wall to infinity). Approximations are still required using this approach, as presented by Moore, Buchwald, and Brewster [8] for a Stokesian entry problem, in which the remaining wall translates, and by Kim, Choi, and Jeong [9] for a model of the half-pitot tube, in which a shear flow is prevented from generating any flux into the channel. The following study is both an application

*Received by the editors September 19, 2007; accepted for publication (in revised form) January 14, 2008; published electronically May 2, 2008.
http://www.siam.org/journals/siap/68-5/70321.html
†Department of Mathematics, University of Manchester, Manchester M13 9PL, UK (i.d.abrahams@manchester.ac.uk).
‡Department of Mechanical and Aerospace Engineering, Jacobs School of Engineering, UCSD, La Jolla, CA 92093-0411 (amdavis@ucsd.edu, sgls@ucsd.edu).

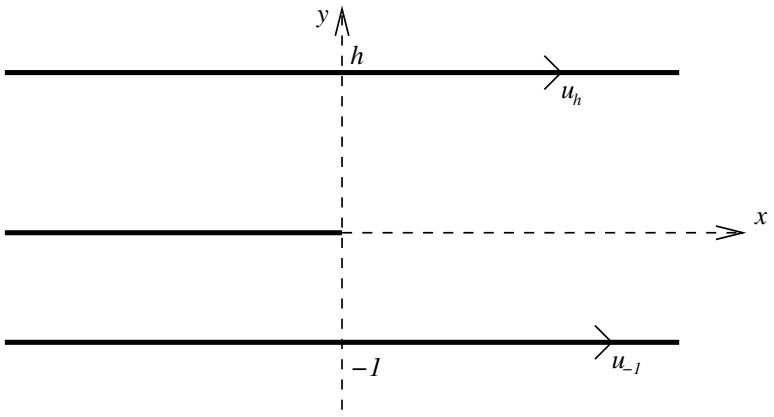


FIG. 1.1. *Geometry of problem.*

of a new Padé approximant procedure [10] and the first solution of this classic problem by the Wiener–Hopf technique.

Consider the unidirectional flow between rigid walls at $y = -1$, $h$, where $(x, y)$ are Cartesian coordinates, at which the velocity $u$ has the prescribed values $u_{-1}$, $u_h$, respectively (see Figure 1.1). The flow $u^\infty(y)\hat{\mathbf{x}}$, where $\hat{\mathbf{x}}$ is the unit vector in the $x$ direction, is given by

$$u^\infty(y) = u_h\left(\frac{y+1}{h+1}\right) + u_{-1}\left(\frac{h-y}{h+1}\right) - \frac{G}{2\mu}(h-y)(y+1). \tag{1.1}$$

Here the first two terms of the velocity profiles may be identified as a shear flow with different wall speeds and the last term with a flow driven by a pressure gradient $G$ that accounts for the prescribed flux being different from the flux generated by the shear flow. It is readily observed from (1.1) that only the weighted average of the wall velocities has a role in the study of the disturbance flow generated by the introduction of a fixed plate at $y = 0, x < 0$. With $u_h + u_{-1}h = -U(h+1)$, this occurs when the flow speed at $y = 0$, namely

$$u^\infty(0) = \frac{u_h + u_{-1}h}{h+1} - \frac{Gh}{2\mu} = -\left(U + \frac{Gh}{2\mu}\right), \tag{1.2}$$

is nonzero, or when there is a flux "mismatch" in $(-1, 0)$ between the upstream flow and that in the downstream channel.

In terms of pressure gradients $G_-$, $G_+$ at infinity (as shown in Figure 1.1), the downstream ($x \to -\infty$) unidirectional velocity profiles are given by

$$u_-^\infty(y) = -u_{-1}y + \frac{G_-}{2\mu}y(y+1), \qquad -1 < y < 0, \tag{1.3}$$

$$u_+^\infty(y) = u_h\frac{y}{h} - \frac{G_+}{2\mu}y(h-y), \qquad 0 < y < h, \tag{1.4}$$

whose total flux must equal that in the upstream ($x \to \infty$) unidirectional velocity profile (1.1). Thus

$$\frac{(G_+ - G)h^3 + (G_- - G)}{6\mu} = (h+1)\left(U + \frac{Gh}{2\mu}\right), \tag{1.5}$$

which is to be viewed as determining the upstream pressure gradient $G$ in terms of $G_+, G_-, U$. The flux "mismatch," $\Delta Q$, is now given by

$$\Delta Q = \int_{-1}^{0} \left[u^\infty(y) - u_-^\infty(y)\right] dy = -\frac{1}{2}\left(U + \frac{Gh}{2\mu}\right) + \frac{(G_- - G)}{12\mu}. \tag{1.6}$$

Evidently the sets of values of the wall velocities and pressure gradients in (1.1), (1.3) for which the presence of the semi-infinite barrier creates a disturbance flow form a two-parameter family described by nonzero values of the vector $[u^\infty(0), \Delta Q]$, with only its direction being significant. Thus any two flows of type (1.1), (1.3) that yield parallel values of this vector, determined by (1.2), (1.6), may be regarded as equivalent because their suitably weighted difference must be a unidirectional flow with zero velocity at $y = 0$.

For example, the two flows determined by $G_- = 0 = G$ and either $u_{-1} = 0, u_h = V^*$ or $u_{-1} = -V, u_h = 0$ both yield values of $[u^\infty(0), \Delta Q]$ that are parallel to $(2, 1)$ because, if $V^* = -Vh$, they differ by the shear flow $u = Vy$. The former is the finite version of the two-dimensional model of a half-pitot tube studied by Kim, Choi, and Jeong [9], whose motivation was the experimental work reported by Stanton, Marshall, and Bryant [11] and Taylor [12]. The latter is the finite version of a Stokesian entry problem, with no pressure gradient far down the semi-infinite channel, studied by Moore, Buchwald, and Brewster [8]. The condition of no pressure gradient upstream ensures, for any $u_h$, that their flow is recovered in the limit $h \to \infty$.

In the case of symmetric geometry, $h = 1$ and evidently (1.2)–(1.6) show that flows with $u_{-1} = -U = u_h$, $G_+ = G_-$ are equivalent to the even case:

$$\Delta Q = 0, \quad u_-^\infty(-y) = u_+^\infty(y), \quad 0 < y < 1, \tag{1.7}$$

which consists downstream of a shear and pressure-driven flow combination, while flows with $u_{-1} = 0 = u_h$, $G_+ = -G_-$ are equivalent to the odd case:

$$G = 0, \quad u^\infty(0) = 0, \quad \Delta Q = \frac{G_-}{12\mu}, \quad u_-^\infty(-y) = -u_+^\infty(y), \quad 0 < y < 1, \tag{1.8}$$

which is a pressure-driven flow out of one channel into the other.

In view of the above discussion, a generic study which covers *all possible* flow cases in fact need only consider forcing due solely to the moving walls and various combinations of downstream pressure gradients. The two cases are therefore the following:

1. $U \neq 0$ and $G_+ = 0 = G_-$. Therefore, $[u^\infty(0), \Delta Q]$ is parallel to $[2(h^2 - h + 1), h(h-1)]$, so its direction depends on $h$ only.
2. $U = 0$ and various flux ratios. Hence

$$\frac{\Delta Q}{u^\infty(0)} = \frac{3h + 1 - G_-/G}{6h}, \tag{1.9}$$

which displays a two-parameter dependence.

As an illustration of the use of MATLAB, a computational solution of this channel flow, using approximate boundary conditions, was given by Fehribach and Davis [13].

**2. The Wiener–Hopf problem.** The equations of steady creeping flow, the Stokes equations [14], are

$$\nabla p = \mu \nabla^2 \mathbf{v}, \qquad \nabla \cdot \mathbf{v} = 0, \tag{2.1}$$

where $\mathbf{v}$ is the velocity, $p$ the dynamic pressure, and $\mu$ the viscosity. For two-dimensional flow referred to Cartesian coordinates $(x, y)$, equations (2.1) allow a stream function $\psi(x, y)$ to be introduced such that

$$\mathbf{v} = \frac{\partial \psi}{\partial y}\hat{\mathbf{x}} - \frac{\partial \psi}{\partial x}\hat{\mathbf{y}}, \qquad \nabla^4 \psi = 0. \tag{2.2}$$

Consider the flow between rigid walls at $y = -1$, $h$ and a semi-infinite fixed barrier at $y = 0$, $x < 0$ at which the stream function has distinct constant values and its $y$-derivative has the prescribed values $u_{-1} = -U$, $u_h = -U$, 0, respectively (see Figure 1.1). Then $\mathbf{v} \sim u^{\infty}(y)\hat{\mathbf{x}}$ as $x \to \infty$ and $\mathbf{v} \sim u^{\infty}_{\pm}(y)\hat{\mathbf{x}}$ as $x \to -\infty$, where $u^{\infty}(y)$ and $u^{\infty}_{\pm}(y)$ are given by (1.1) and (1.3), (1.4), with the upper "plus" (lower "minus") sign referring to the upper (lower) duct region. It is advantageous to choose for the disturbance field not $\mathbf{v} - u^{\infty}(y)\hat{\mathbf{x}}$ but rather $\mathbf{v} - u^{\infty}_{\pm}(y)\hat{\mathbf{x}}$. Thus, on setting, as in (2.2),

$$\mathbf{v} - u^{\infty}_{\pm}(y)\hat{\mathbf{x}} = \frac{\partial \bar{\psi}}{\partial y}\hat{\mathbf{x}} - \frac{\partial \bar{\psi}}{\partial x}\hat{\mathbf{y}}, \qquad \begin{cases} 0 < y < h, \\ -1 < y < 0, \end{cases} \tag{2.3}$$

the disturbance stream function $\bar{\psi}(x, y)$ is biharmonic, satisfies the homogeneous conditions

$$\bar{\psi} = 0 = \frac{\partial \bar{\psi}}{\partial y} \text{ at } y = -1, h, \quad -\infty < x < \infty, \quad \text{and } y = 0, \quad x < 0, \tag{2.4}$$

is continuous along with its $y$-derivative on $y = 0$, $x > 0$, and, according to (1.3), (1.4), and (2.3), is generated by the discontinuities

$$\left[\frac{\partial^2 \bar{\psi}}{\partial y^2}\right]_{0-}^{0+} = U\frac{h+1}{h} + \frac{G_+ h + G_-}{2\mu}, \qquad \left[\frac{\partial^3 \bar{\psi}}{\partial y^3}\right]_{0-}^{0+} = -\frac{G_+ - G_-}{\mu} \tag{2.5}$$

on $y = 0, x > 0$. If, for convenience, these discontinuities tend to zero as $x \to \infty$, i.e., (2.5) is modified to

$$\left[\frac{\partial^2 \bar{\psi}}{\partial y^2}\right]_{0-}^{0+} = \left[U\frac{h+1}{h} + \frac{G_+ h + G_-}{2\mu}\right] e^{-\epsilon x}, \qquad \left[\frac{\partial^3 \bar{\psi}}{\partial y^3}\right]_{0-}^{0+} = -\frac{G_+ - G_-}{\mu} e^{-\epsilon x} \tag{2.6}$$

on $y = 0, x > 0$, where $\epsilon$ is a small positive real constant, then the disturbance stream function $\bar{\psi}$ and its derivatives tend to zero as $x \to \pm\infty$ as a consequence of the choice (2.3), which further implies that the unknown functions $s(x)$, $t(x)$, defined by

$$\left[\frac{\partial^2 \bar{\psi}}{\partial y^2}\right]_{0-}^{0+} = s(x), \quad \left[\frac{\partial^3 \bar{\psi}}{\partial y^3}\right]_{0-}^{0+} = t(x), \quad y = 0, \quad x < 0, \tag{2.7}$$

also decay to zero as $x \to -\infty$. On completion of the solution procedure $\epsilon$ will be set to zero.

In terms of the Fourier transform

$$\Psi(k, y) = \int_{-\infty}^{\infty} \bar{\psi}(x, y) e^{ikx} dx, \tag{2.8}$$

the boundary conditions (2.4), (2.6), (2.7) yield

$$\Psi(k, -1) = 0 = \Psi_y(k, -1), \qquad \Psi(k, h) = 0 = \Psi_y(k, h), \tag{2.9}$$

$$\Psi(k,0)=\int_0^\infty \bar\psi(x,0)e^{ikx}dx=\Psi^+(k,0),\qquad \Psi_y(k,0)=\Psi_y^+(k,0), \tag{2.10}$$

$$\begin{aligned}[\Psi_{yy}(k,y)]_{0-}^{0+}&=\int_{-\infty}^0 s(x)e^{ikx}dx+\left[U\frac{h+1}{h}+\frac{G_+h+G_-}{2\mu}\right]\int_0^\infty e^{ix(k+i\epsilon)}dx\\&=S^-(k)+\left[U\frac{h+1}{h}+\frac{G_+h+G_-}{2\mu}\right]\frac{i}{k+i\epsilon},\end{aligned} \tag{2.11}$$

$$\begin{aligned}[\Psi_{yyy}(k,y)]_{0-}^{0+}&=\int_{-\infty}^0 t(x)e^{ikx}dx-\frac{G_+-G_-}{\mu}\int_0^\infty e^{ix(k+i\epsilon)}dx\\&=T^-(k)-\frac{G_+-G_-}{\mu}\frac{i}{k+i\epsilon}.\end{aligned} \tag{2.12}$$

Convergence of the above Fourier full- and half-range transforms is ensured if $k$ lies in an infinite strip containing the real line, here and henceforth referred to as $\mathcal{D}$, with its width limited from below by the singularity at $k=-i\epsilon$. Evidently (see [1]) the unknown pairs of (half-range transform) functions $\Psi^+(k,0)$, $\Psi_y^+(k,0)$ and $S^-(k)$, $T^-(k)$ are regular in the region above and including $\mathcal{D}$, denoted $\mathcal{D}^+$, and the region below and including $\mathcal{D}$, denoted $\mathcal{D}^-$, respectively. Thus, $\mathcal{D}^+\cap\mathcal{D}^-\equiv\mathcal{D}$.

In view of the behavior of $\bar\psi$ at $x=\pm\infty$, the Fourier transform (2.8) can be applied to the biharmonic equation, whence

$$\left(\frac{d^2}{dy^2}-k^2\right)^2\Psi=0 \tag{2.13}$$

and hence a general solution which satisfies (2.9) is

$$\begin{aligned}\Psi(k,y)&=A(k)k(1+y)\sinh[k(1+y)]\\&\quad+B(k)\{k(1+y)\cosh[k(1+y)]-\sinh[k(1+y)]\},\qquad -1<y<0,\end{aligned} \tag{2.14}$$

$$\begin{aligned}\Psi(k,y)&=C(k)k(h-y)\sinh[k(h-y)]\\&\quad+D(k)\{k(h-y)\cosh[k(h-y)]-\sinh[k(h-y)]\},\qquad 0<y<h.\end{aligned} \tag{2.15}$$

Application of the conditions (2.10) now yields

$$\begin{aligned}\begin{pmatrix}A(k)\\B(k)\end{pmatrix}&=\frac{1}{\sinh^2 k-k^2}\\&\times\begin{pmatrix}k\sinh k & -(k\cosh k-\sinh k)\\-(k\cosh k+\sinh k) & k\sinh k\end{pmatrix}\begin{pmatrix}\Psi^+(k,0)\\k^{-1}\Psi_y^+(k,0)\end{pmatrix},\end{aligned} \tag{2.16}$$

$$\begin{aligned}\begin{pmatrix}C(k)\\D(k)\end{pmatrix}&=\frac{1}{\sinh^2 kh-k^2h^2}\\&\times\begin{pmatrix}kh\sinh kh & kh\cosh kh-\sinh kh\\-(kh\cosh kh+\sinh kh) & -kh\sinh kh\end{pmatrix}\begin{pmatrix}\Psi^+(k,0)\\k^{-1}\Psi_y^+(k,0)\end{pmatrix}.\end{aligned} \tag{2.17}$$

As $\Psi^+(k,y)$ and $\Psi_y^+(k,y)$ are continuous across the line $y=0$, the discontinuities (2.11), (2.12) may be regarded as conditions on $\Psi_{yy}-k^2\Psi$ and its derivative, which facilitates the deduction of the following *matrix* Wiener–Hopf equation:

$$\begin{pmatrix}T^-(k)\\-S^-(k)\end{pmatrix}-\frac{i}{k+i\epsilon}\left(U\frac{h+1}{h}\begin{bmatrix}0\\1\end{bmatrix}+\frac{1}{2\mu}\begin{bmatrix}2G_+-2G_-\\G_+h+G_-\end{bmatrix}\right)=\mathbf{K}(k)\begin{pmatrix}\Psi^+(k,0)\\\Psi_y^+(k,0)\end{pmatrix}, \tag{2.18}$$

where

$$\mathbf{K}(k) = \begin{pmatrix} k^2[f(k)+g(k)] & -ke(k) \\ -ke(k) & g(k)-f(k) \end{pmatrix}, \tag{2.19}$$

$$e(k) = 2k\left(\frac{k^2}{\sinh^2 k - k^2} - \frac{k^2h^2}{\sinh^2 kh - k^2h^2}\right), \tag{2.20}$$

$$f(k) = 2k\left(\frac{k}{\sinh^2 k - k^2} + \frac{kh}{\sinh^2 kh - k^2h^2}\right), \tag{2.21}$$

$$g(k) = k\left[\frac{\sinh 2k}{\sinh^2 k - k^2} + \frac{\sinh 2kh}{\sinh^2 kh - k^2h^2}\right]. \tag{2.22}$$

It can easily be seen that $\mathbf{K}(k)$ possesses the properties

$$\mathbf{K}(k) = \mathbf{K}(-k) = [\mathbf{K}(k)]^T, \tag{2.23}$$

where $T$ denotes the transpose, a fact that is exploited subsequently. The determinant of the kernel is

$$|\mathbf{K}(k)| = \frac{4k^4[\sinh^2 k(h+1) - k^2(h+1)^2]}{(\sinh^2 kh - k^2h^2)(\sinh^2 k - k^2)}. \tag{2.24}$$

The forcing term in (2.18) displays the two independent flows identified above. In the case of symmetric geometry, $h = 1$ implies that $e(k)$ is identically zero, and hence the Wiener–Hopf equation (2.18) separates into disjoint scalar equations of standard type. Then, in the even case, $G_+ \equiv G_-$ implies that $T^-$ and $\Psi^+$ vanish, while, in the odd case, $U \equiv 0 \equiv G_+ + G_-$ implies that $S^-$ and $\Psi_y^+$ vanish, as expected.

It remains to consider the pressure singularity at the barrier edge. In the neighborhood of $r = 0$, using the obvious polar coordinate representation,

$$\bar{\psi} \sim 2^{1/2} r^{3/2} \cos\frac{1}{2}\theta[\Lambda_1 \sin\theta + \Lambda_2(1+\cos\theta)] \tag{2.25}$$

$$= \Lambda_1(r+x)^{1/2} y + \Lambda_2(r+x)^{3/2}, \tag{2.26}$$

after rejecting the more singular terms of order $r^{1/2}$. Thus

$$\bar{\psi}(x,0) \sim \Lambda_2(2x)^{3/2}, \qquad \frac{\partial\bar{\psi}}{\partial y}(x,0) \sim \Lambda_1(2x)^{1/2} \text{ as } x \to 0+, \tag{2.27}$$

and by writing, for $x < 0$,

$$\bar{\psi} \sim \frac{\Lambda_1 y|y|}{(r-x)^{1/2}} + \frac{\Lambda_2|y|^3}{(r-x)^{3/2}}; \tag{2.28}$$

it follows that

$$\frac{\partial^2\bar{\psi}}{\partial y^2}(x,0) \sim \pm\Lambda_1\left(\frac{2}{-x}\right)^{1/2}, \qquad \frac{\partial^3\bar{\psi}}{\partial y^3}(x,0) \sim \pm\Lambda_2\frac{6}{(-2x)^{3/2}} \tag{2.29}$$

as $x \to 0-$ on the upper/lower side of the barrier. The latter result indicates that the pressure jump across the barrier behaves as $6\mu\Lambda_2(2/(-x))^{1/2}$ as the edge is approached. This agrees with the asymptotic form

$$\mu^{-1}\bar{p} \sim 2^{1/2} r^{-1/2} \left( -\Lambda_1 \cos\frac{1}{2}\theta + 3\Lambda_2 \sin\frac{1}{2}\theta \right), \tag{2.30}$$

obtained from (2.25) by noting that (2.1) and (2.2) ensure that $\bar{p}$ and $\mu\nabla^2\bar{\psi}$ are conjugate functions. The rejection of order $r^{1/2}$ terms in (2.25) thus minimizes the *order* of this edge singularity in the pressure, as, for example, in the calculations for the spherical cap [15] and the hollow sphere with caps removed [16]. A bounded pressure jump occurs if $\Lambda_2 = 0$, which may be achieved by a suitable choice of the direction of the forcing vector in (2.18). Such a procedure is unnecessary for the geometrically symmetric even case since then $\Lambda_2$ must be zero for $\bar{\psi}$ to be an odd function of $\theta$ in (2.25). The Wiener–Hopf calculation [2, 3, 5] generates an entire function that is identically zero, from which it is deduced that $\Lambda_1 = 2/\sqrt{\pi}$.

## 3. Factorization of the duct kernel.

**3.1. Introduction and overview of the factorization procedure.** In the previous section the matrix Wiener–Hopf equation was derived, in which the kernel, $\mathbf{K}(k)$, is written in (2.19). The aim of this section is to factorize $\mathbf{K}(k)$ into a product of two matrices

$$\mathbf{K}(k) = \mathbf{K}^-(k)\mathbf{K}^+(k), \tag{3.1}$$

one containing those singularities of $\mathbf{K}(k)$ lying in the lower half-plane, referred to as $\mathbf{K}^+(k)$, and $\mathbf{K}^-(k)$, which is analytic in the lower half-plane $\mathcal{D}^-$ and hence contains the singularities of $\mathbf{K}(k)$ lying above the strip $\mathcal{D}$. Note that $[\mathbf{K}^+(k)]^{-1}$ and $[\mathbf{K}^-(k)]^{-1}$ are also analytic in the regions $\mathcal{D}^+$ and $\mathcal{D}^-$, respectively. Further, it is necessary for successful completion of the Wiener–Hopf procedure that $\mathbf{K}^{\pm}(k)$ are at worst of algebraic growth (see Noble [1]). Unfortunately, although matrix kernel factorization with the requisite growth behavior has been proven to be possible for a wide class of kernels (Gohberg and Krein [17]), to which the kernel (2.19) belongs, no constructive method has been found to complete this in general. There are classes of matrices for which product factorization can be achieved explicitly, the most important of which are those amenable to Hurd's method [18] and Khrapkov–Daniele commutative matrices [19, 20]. Details of these, and an extensive bibliography on matrix kernel factorization, can be found in [21, 10, 22]. The present problem yields a kernel which, to the authors' knowledge, falls outside of the classes permitting an exact factorization, and so an approximate decomposition will be performed here. The approach follows that developed recently by one of the authors and has been successfully applied to problems in elasticity [21, 22] and acoustics [10]. Essentially, the procedure is to rearrange the kernel into an appropriate form, namely, to resemble a Khrapkov (commutative) matrix, and then to replace a scalar component of it by a function which approximates it accurately in the strip of analyticity $\mathcal{D}$. The new approximate kernel is able to be factorized exactly (into an explicit noncommutative decomposition), and, in the previous cases cited above, strong numerical evidence was offered for convergence of the resulting approximate factors to the exact ones as the scalar approximator is increased in accuracy. Further, the convergence to the solution has been validated for one particular matrix kernel [23], where an *exact* noncommutative factorization can be derived by an alternative procedure.

The kernel in (2.19) appears, on face value, significantly simpler to factorize than those in the previously mentioned articles [21, 10], because it contains only simple pole singularities rather than branch cuts. Therefore, it could perhaps be considered as more appropriately factorized by pole removal methods, such as those suggested

by Idemen [24], Noble [1], Rawlins [25], Abrahams [26], and Abrahams and Wickham [27], reducing the problem down to an infinite algebraic system of equations which needs to be solved numerically. However, there are three reasons why this approach is not useful here. The first is a technical point; it can be shown that the procedure for removing singularities from the kernel, and thereby obtaining the kernel factors $\mathbf{K}^{\pm}(k)$, is not nearly as straightforward as for those kernels considered by the aforementioned authors. Second, the pole locations are complex and are found from the zeros of the determinant of the kernel $\mathbf{K}(k)$ in (2.24), i.e., the roots of the transcendental Papkovich–Fadle dispersion relation. This creates further complications in the factorization scheme. The third, and most compelling, reason for avoiding this approach is that we would like a final solution which will offer *uniformly* accurate results for all values of upper duct height $h$, from $h = 1$ to $h = \infty$, a range that does not imply any loss of generality. Clearly, as $h \to \infty$, more and more of the Papkovich–Fadle poles need to be included to maintain constant accuracy (more and more move down close to the strip $\mathcal{D}$), and so the corresponding algebraic system to solve has to be truncated after a greater and greater number of terms. Thus, we cannot expect to recover the $h \to \infty$ case, that is, when the upper duct top wall is removed, so we could not employ such a factorization in a solution which we would hope to compare with other results for this particular flow domain (Moore, Buchwald, and Brewster [8], Kim, Choi, and Jeong [9], etc.)

In view of the above arguments we aim to employ the Wiener–Hopf approximant matrix (WHAM) method [10] discussed previously and to do this in such a way that maintains the requisite accuracy over all values of $h \geq 1$. As mentioned in the introduction, when $h = 1$, then the kernel should reduce to two scalar functions, reflecting the symmetric and antisymmetric motions clearly evident to exist from the symmetry in duct geometry. When $h = \infty$, the upper duct wall is removed, and although others have tackled this by alternative approximate/numerical means, it can, in fact, be shown that the kernel actually reduces to a commutative (Khrapkov) form [23]. Therefore, an exact factorization is again achievable. Hence, if the approximate factorization, to be achieved here by the WHAM method, is organized so that in both limits, $h \to 1$ and $h \to \infty$, it reduces to the exact kernel decomposition, then very good accuracy can be expected for all intermediate $h$ values. This is what will be done below. However, as a complication to this factorization, we must take account of two unfortunate features of the kernel. The first is the fact that the elements of $\mathbf{K}(k)$, and in particular $e(k)$, $f(k)$ shown in (2.20)–(2.22), differ by a factor of $k$ near the origin. This is identical to that found for the kernel in [21] and can be handled by a suitable rearrangement of terms. The second is due to the fact that $\mathbf{K}(k)$ must be written as a product of three matrices such that the inner matrix $\mathbf{L}(k)$ (see (3.6) below) has a determinant with behavior proportional to $k^{-2}$ as $k \to 0$. This is a removable singularity because it is pre- and postmultiplied by matrices which each have determinant $k$. Unfortunately, the inner matrix is the one we initially factorize, and so additional arrangement is necessary to take this small-$k$ behavior into account. With these points of explanation in mind, the factorization procedure is now elucidated.

### 3.2. Conditioning of the matrix kernel.

**3.2.1. Behavior for large $|k|$.** The matrix $\mathbf{K}(k)$ is characterized by its elements $e(k)$, $f(k)$, $g(k)$, given in (2.20)–(2.22), and in particular by their behavior for large

and small $k$. For large $k$ it is easily deduced that

$$e(k) \sim 8k^3(e^{-2|k|} - h^2 e^{-2|k|h}), \quad |k| \to \infty, \quad k \in \mathcal{D}, \tag{3.2}$$

$$f(k) \sim 8k^2(e^{-2|k|} + he^{-2|k|h}), \quad |k| \to \infty, \quad k \in \mathcal{D}, \tag{3.3}$$

$$g(k) \sim 4|k|, \quad |k| \to \infty, \quad k \in \mathcal{D}. \tag{3.4}$$

It is appropriate to arrange the kernel to be diagonally dominant as $k \to \infty$ in $\mathcal{D}$, and so simple algebra gives

$$\mathbf{K}(k) = \frac{1}{2}\begin{pmatrix} 0 & -k \\ 1 & 0 \end{pmatrix}\begin{pmatrix} 1 & -1 \\ i & i \end{pmatrix}\mathbf{L}(k)\begin{pmatrix} i & 1 \\ i & -1 \end{pmatrix}\begin{pmatrix} k & 0 \\ 0 & 1 \end{pmatrix}, \tag{3.5}$$

where $\mathbf{L}(k)$ may be written in the form

$$\mathbf{L}(k) = g(k)\mathbf{I} + \begin{pmatrix} 0 & f(k) + ie(k) \\ f(k) - ie(k) & 0 \end{pmatrix}, \tag{3.6}$$

with $\mathbf{I}$ the identity.

**3.2.2. Behavior of the kernel near the origin.** Near the origin the scalar functions $e(k)$, $f(k)$, $g(k)$ take the form

$$e(k) \sim 6\left(\frac{h^2 - 1}{h^2}\right)\frac{1}{k}, \tag{3.7}$$

$$f(k) \sim 6\left(\frac{h^3 + 1}{h^3}\right)\frac{1}{k^2}, \tag{3.8}$$

$$g(k) \sim 6\left(\frac{h^3 + 1}{h^3}\right)\frac{1}{k^2}, \tag{3.9}$$

to leading order, and it is easy to show that at the next order

$$g(k) - f(k) \sim 4\left(\frac{h + 1}{h}\right), \tag{3.10}$$

so that we may write

$$g(k) - f(k) \sim \beta^2 k^2 f(k), \tag{3.11}$$

in which

$$\beta^2 = \frac{2}{3}\frac{h^2}{h^2 - h + 1}. \tag{3.12}$$

Note that $\beta^2$ tends to its minimum value $2/3$ as $h \to 1$ or $h \to \infty$ and takes the maximum value $8/9$. This small variation in value over all $h$ is important to ensure an eventually uniform factorization accuracy. We may also express $e(k)$ in terms of $f(k)$ near the origin:

$$e(k) \sim \delta k f(k), \tag{3.13}$$

where the parameter $\delta$ takes the value

$$\delta = \frac{h(h - 1)}{h^2 - h + 1} \tag{3.14}$$

and is monotonic in $h$ going from $\delta = 0$ at $h = 1$ to $\delta = 1$ at $h = \infty$. Again, this small variation will prove helpful to the factorization.

We now arrange $\mathbf{L}(k)$ to appear in Khrapkov form, namely, that the square of the second matrix term should be a scalar polynomial in $k$ times the identity. We can do this by removing the factor $\sqrt{f^2(k) + e^2(k)}$ from this matrix in (3.6). However, as

$$f(k) \pm ie(k) \sim f(k)(1 \pm i\delta k), \qquad k \to 0, \tag{3.15}$$

it is more effective [21] to write $\mathbf{L}(k)$ as

$$\mathbf{L}(k) = g(k)\mathbf{I} + \sqrt{\frac{f^2(k) + e^2(k)}{1 + \delta^2 k^2}}\mathbf{J}(k), \tag{3.16}$$

$$\mathbf{J}(k) = \begin{pmatrix} 0 & d(k)(1 + i\delta k) \\ d^{-1}(k)(1 - i\delta k) & 0 \end{pmatrix}, \tag{3.17}$$

in which

$$d(k) = \sqrt{\left(\frac{f(k) + ie(k)}{f(k) - ie(k)}\right)\left(\frac{1 - i\delta k}{1 + i\delta k}\right)}. \tag{3.18}$$

It is a simple matter to show that we can choose a branch of $d(k)$ which is regular in $\mathcal{D}$, takes the value unity at $k = 0$, and, in view of the relative magnitudes of $e(k)$, $f(k)$ as $|k| \to \infty$ in $\mathcal{D}$, (3.2), (3.3), also tends to unity at infinity in the strip. If we had omitted the factor $(1 - i\delta k)/(1 + i\delta k)$ in $d(k)$, then $\arg(d(k))$ would not have tended to zero as $k \to \pm\infty$.

The matrix $\mathbf{L}(k)$ now appears to be in Khrapkov form, in view of the property

$$\mathbf{J}^2(k) = \Delta^2(k)\mathbf{I}, \tag{3.19}$$

where $\Delta^2(k)$ is the polynomial

$$\Delta^2(k) = 1 + \delta^2 k^2. \tag{3.20}$$

However, $\mathbf{J}(k)$ is not entire, as required for a Khrapkov factorization, but contains $d(k)$, which has infinite sequences of finite branch cuts at rotationally symmetric locations in the upper and lower half-planes. These will have to be considered once the partial Khrapkov decomposition is complete but, for the present, will be ignored.

### 3.3. Partial decomposition of $\mathbf{K}(k)$.

**3.3.1. Limiting values of $\mathbf{L}(k)$.** The first point to remark here is that (3.19) is arranged in appropriate form for the limiting values of $h$. As $h \to 1$, expression (2.20) reveals immediately that $e(k) = 0$ and similarly, from (3.14), $\delta = 0$. Hence $\mathbf{L}(k)$ reduces to

$$\mathbf{L}(k) = g(k)\mathbf{I} + f(k)\begin{pmatrix} 0 & 1 \\ 1 & 0 \end{pmatrix}, \qquad h = 1. \tag{3.21}$$

By adding and subtracting rows this can be trivially reduced to two scalar decomposition problems, but this will also be decomposed *exactly* in the following Khrapkov factorization as $d(k) \equiv 1$. Similarly, as $h \to \infty$, $\delta \to 1$ and

$$e(k) = kf(k) = \frac{2k^3}{\sinh^2 k - k^2}, \qquad h \to \infty. \tag{3.22}$$

Hence in this limit $d(k) = 1$ also and

$$\mathbf{L}(k) = g(k)\mathbf{I} + f(k)\begin{pmatrix} 0 & 1+ik \\ 1-ik & 0 \end{pmatrix}, \qquad h = \infty, \tag{3.23}$$

which also permits an exact factorization [23] and justifies the particular form of $d(k)$ chosen in (3.18).

**3.3.2. Introduction of resolvent matrix.** Before performing the Khrapkov factorization on $\mathbf{L}(k)$, there is a problem, alluded to above, which must be resolved first. Note that as $k \to 0$, from (3.6), (3.11), and (3.13),

$$\mathbf{L}(k) \sim f(k)\begin{pmatrix} 1+\beta^2k^2 & 1+i\delta k \\ 1-i\delta k & 1+\beta^2k^2 \end{pmatrix} \tag{3.24}$$

so that

$$|\mathbf{L}(k)| \sim \left[6\frac{h^3+1}{h^3k^2}\right]^2 (2\beta^2-\delta^2)k^2 \sim \frac{12(h+1)^4}{h^4k^2} + \mathcal{O}(1). \tag{3.25}$$

This is clearly singular at the origin and therefore violates the original assumption of regularity in $\mathcal{D}$. Of course, this is because we are working with $\mathbf{L}(k)$ and not the original kernel $\mathbf{K}(k)$. To overcome this "removable singularity" in the determinant it is convenient to introduce the new matrix, $\mathbf{R}(k)$, called the resolvent, where

$$\mathbf{R}^{-1}(k) = (1+\beta^2k^2)\mathbf{I} - \mathbf{J}(k), \tag{3.26}$$

with $\mathbf{J}(k)$ as in (3.17), which commutes with $\mathbf{L}(k)$. The combined matrix

$$\mathbf{T}(k) = \mathbf{R}^{-1}(k)\mathbf{L}(k) \tag{3.27}$$

has determinant value

$$\left[\frac{2(h+1)^3}{h(h^2-h+1)}\right]^2 \tag{3.28}$$

at $k = 0$, and so $\mathbf{T}(k)$ may now be factorized instead of $\mathbf{L}(k)$. We will later have to deal with factorizing $\mathbf{R}(k)$, but this will not prove to be a problem.

**3.3.3. Partial decomposition of matrix $\mathbf{T}(k)$.** We have seen above that $\mathbf{R}^{-1}(k)$ and $\mathbf{L}(k)$ commute, and indeed any matrices of the form $\alpha\mathbf{I} + \beta\mathbf{J}(k)$ will commute with any other. Therefore, we may pose (see [19]) the product factors of $\mathbf{T}(k)$ in the form

$$\mathbf{T}^{\pm}(k) = r^{\pm}(k)\left(\cosh[\Delta(k)\theta^{\pm}(k)]\mathbf{I} + \frac{1}{\Delta(k)}\sinh[\Delta(k)\theta^{\pm}(k)]\mathbf{J}(k)\right), \tag{3.29}$$

where $r^{\pm}(k)$, $\theta^{\pm}(k)$ are scalar functions of $k$ with the analyticity property indicated by their superscript. The function $\Delta(k)$, given by (3.20), generates no branch cuts because (3.29) contains only even powers of $\Delta(k)$. The scalar factors $r^{\pm}(k)$, $\theta^{\pm}(k)$ are deduced by equating

$$\mathbf{T}(k) = \mathbf{T}^{+}(k)\mathbf{T}^{-}(k), \tag{3.30}$$

which yields

$$r^+(k)r^-(k)\cosh[\Delta(k)(\theta^+(k)+\theta^-(k))] = g(1+\beta^2k^2) - \Delta\sqrt{f^2+e^2}, \tag{3.31}$$

$$r^+(k)r^-(k)\sinh[\Delta(k)(\theta^+(k)+\theta^-(k))] = \sqrt{f^2+e^2}(1+\beta^2k^2) - \Delta g. \tag{3.32}$$

These may be separated to give

$$[r^+(k)r^-(k)]^2 = (g^2-f^2-e^2)\left[(2\beta^2-\delta^2)+\beta^4k^2\right]k^2, \tag{3.33}$$

$$\tanh[\Delta(k)(\theta^+(k)+\theta^-(k))] = \frac{\sqrt{f^2+e^2}(1+\beta^2k^2)-\Delta g}{g(1+\beta^2k^2)-\Delta\sqrt{f^2+e^2}}, \tag{3.34}$$

and by the usual sum-split formula (e.g., equation (1.17) of Noble [1])

$$\begin{aligned}\theta^+(k) &= \frac{1}{2\pi i}\int_{-\infty}^{\infty}\frac{1}{\Delta(\zeta)}\tanh^{-1}\left\{\frac{\sqrt{f^2(\zeta)+e^2(\zeta)}(1+\beta^2\zeta^2)-\Delta(\zeta)g(\zeta)}{g(\zeta)(1+\beta^2\zeta^2)-\Delta(\zeta)\sqrt{f^2(\zeta)+e^2(\zeta)}}\right\}\frac{d\zeta}{\zeta-k}\\ &= \frac{k}{\pi i}\int_0^{\infty}\frac{1}{\Delta(\zeta)}\tanh^{-1}\left\{\frac{\sqrt{f^2(\zeta)+e^2(\zeta)}(1+\beta^2\zeta^2)-\Delta(\zeta)g(\zeta)}{g(\zeta)(1+\beta^2\zeta^2)-\Delta(\zeta)\sqrt{f^2(\zeta)+e^2(\zeta)}}\right\}\frac{d\zeta}{\zeta^2-k^2},\end{aligned} \tag{3.35}$$

valid for $\Im(k) > 0$. Note that the last result is true because the integrand is even in $\zeta$, and this further implies that

$$\theta^-(k) = \theta^+(-k), \qquad k \in \mathcal{D}^-. \tag{3.36}$$

Actually, the full range integral could be taken along any path in $\mathcal{D}$ parallel to the real axis, and so if $\theta^+(k)$ is required for real $k$, then the first integral would be indented below (above for $\theta^-(k)$) this point. We can confirm that the integral representations in (3.35) exist by examining the integrand as $\zeta \to 0$ and $\zeta \to \infty$ (it is finite valued at all other points in $\mathcal{D}$). From (3.7)–(3.9) a little algebra reveals that the right-hand side of (3.34) is $\mathcal{O}(k^2)$, $k \to 0$, and similarly (3.2)–(3.4) suggests that (3.34) is $\mathcal{O}(k^{-1})$, $k \to \infty$. Hence, the first integrand in (3.35) is bounded in $\mathcal{D}$ and decays proportionally to $\mathcal{O}(\zeta^{-3})$ as $|\zeta| \to \infty$ in the strip. Therefore, this representation is ideal for computing $\theta^{\pm}(k)$ and can be directly coded for numerical evaluation.

This procedure has to be modified for $[r^+(k)r^-(k)]^2$ in (3.33) whose right-hand side tends to $[2(h+1)^3/h(h^2-h+1)]^2$ as $k \to 0$ and $\sim 16\beta^4k^6$ as $|k| \to \infty, k \in \mathcal{D}$. The latter behavior is not suitable for direct application of the product decomposition formula (Noble [1, equation (1.20)]), which requires a function that tends to the value unity at infinity. This is simply circumvented by applying a suitable divisor to (3.33), employing the standard factorization formula, and then decomposing the divisor into upper- and lower-half functions by inspection. This yields

$$\begin{aligned}r^+(k) = &\left[3^{1/2}\left(\frac{h+1}{h}\right)-2ik\right]^{1/2}\left[3^{1/4}\left(\frac{h+1}{h}\right)(1+i)-2ik\right]^{1/2}\\ &\times\left[3^{1/4}\left(\frac{h+1}{h}\right)(1-i)-2ik\right]^{1/2}\frac{h}{[3(h^2-h+1)]^{1/2}}\\ &\times\exp\left\{\frac{1}{4\pi i}\int_{-\infty}^{\infty}\log\left[\frac{[g^2(\zeta)-f^2(\zeta)-e^2(\zeta)]\zeta^2}{12\left(\frac{h+1}{h}\right)^4+16\zeta^4}\right]\frac{d\zeta}{\zeta-k}\right\}\end{aligned} \tag{3.37}$$

for $\Im(k) > 0$, and indentation of the contour below $k$ is taken if $k$ is real. Note that the exponential function in this expression may be reexpressed as

$$\exp\left\{\frac{k}{2\pi i}\int_0^\infty \log\left[\frac{[g^2(\zeta)-f^2(\zeta)-e^2(\zeta)]\zeta^2}{12\left(\frac{h+1}{h}\right)^4+16\zeta^4)}\right]\frac{d\zeta}{\zeta^2-k^2}\right\}, \tag{3.38}$$

where convergence of this and the above integral are now ensured. The function $r^-(k)$, analytic in the lower half-plane, is again, due to the symmetry, simply obtained from

$$r^-(-k) = r^+(k), \qquad k \in \mathcal{D}^+. \tag{3.39}$$

Hence $\mathbf{T}^\pm(k)$ have been determined (see (3.29), (3.35), (3.37)) in a form which can be evaluated directly, and these are analytic in their indicated half-planes, $\mathcal{D}^\pm$, except for the singularities occurring in $\mathbf{K}(k)$ (due to $d(k)$) which have yet to be resolved.

**3.3.4. Partial decomposition of the resolvent matrix.** Having introduced the inverse of $\mathbf{R}(k)$ above in order to improve the convergence of $\mathbf{L}(k)$, we now need to factorize it directly. The form of $\mathbf{R}(k)$ has been chosen to enable us to do this easily. First, $\mathbf{R}^{-1}(k)$ may, by inspection, be written in the form

$$\frac{1}{2}[(1+ik\sqrt{2\beta^2-\delta^2})\mathbf{I}-\mathbf{J}(k)][(1-ik\sqrt{2\beta^2-\delta^2})\mathbf{I}-\mathbf{J}(k)], \tag{3.40}$$

where both matrices are entire save for the finite cuts in the scalar function $d(k)$ contained within $\mathbf{J}(k)$. The first matrix has determinant

$$-2\beta^2 k(k-i\gamma), \tag{3.41}$$

where

$$\gamma = \frac{\sqrt{2\beta^2-\delta^2}}{\beta^2} = \frac{\sqrt{3}}{2}\left(\frac{h+1}{h}\right), \tag{3.42}$$

and the second has determinant

$$-2\beta^2 k(k+i\gamma). \tag{3.43}$$

Hence we may write

$$\mathbf{R}(k) = 2\mathbf{R}^+(k)\mathbf{R}^-(k), \tag{3.44}$$

where

$$\mathbf{R}^\pm(k) = \frac{1}{2\beta^2 k(k\pm i\gamma)}\left[(1\mp ik\beta^2\gamma)\mathbf{I}+\mathbf{J}(k)\right] \tag{3.45}$$

are the partial decomposition matrices; i.e., they are analytic in their indicated half-planes except for poles at $k=0$ and the finite branch cuts in $d(k)$. Note that $\mathbf{R}^\pm(k)$ commute with each other and with $\mathbf{T}^\pm(k)$, while the pole at $k=i\gamma$ lies in the upper half-plane. Hence, this completes the partial product factorization of $\mathbf{K}(k)$, and from (3.5), (3.27), (3.30), (3.44), we obtain

$$\mathbf{K}(k) = \mathbf{Q}^-(k)\mathbf{Q}^+(k), \tag{3.46}$$

where

$$\mathbf{Q}^-(k) = \begin{pmatrix} -ik & -ik \\ 1 & -1 \end{pmatrix} \mathbf{R}^-(k)\mathbf{T}^-(k), \tag{3.47}$$

$$\mathbf{Q}^+(k) = \mathbf{T}^+(k)\mathbf{R}^+(k) \begin{pmatrix} ik & 1 \\ ik & -1 \end{pmatrix}. \tag{3.48}$$

Note that $\mathbf{Q}^{\pm}(k)$ are free of a pole singularity at $k = 0$ even though $\mathbf{R}^{\pm}(k)$ contain this singularity (verified in section 3.4.3). All that remains is to remove (approximately) the residual singularities appearing in $\mathbf{J}(k)$.

### 3.4. Approximate factorization.

**3.4.1. Padé approximation and partial decomposition of approximate kernel.** There is no exact procedure known for eliminating the finite branch cuts in $d(k)$ from the upper (lower) half-planes of the matrix factor $\mathbf{Q}^+(k)$ ($\mathbf{Q}^-(k)$). To obtain an approximate factorization we replace the original matrix $\mathbf{K}(k)$ by a new one, $\mathbf{K}_N(k)$, where

$$\mathbf{K}_N(k) = \frac{1}{2} \begin{pmatrix} 0 & -k \\ 1 & 0 \end{pmatrix} \begin{pmatrix} 1 & -1 \\ i & i \end{pmatrix} \mathbf{L}_N(k) \begin{pmatrix} i & 1 \\ i & -1 \end{pmatrix} \begin{pmatrix} k & 0 \\ 0 & 1 \end{pmatrix}, \tag{3.49}$$

$$\mathbf{L}_N(k) = g(k)\mathbf{I} + \sqrt{\frac{f^2(k) + e^2(k)}{1 + \delta^2 k^2}}\mathbf{J}_N(k), \tag{3.50}$$

and $\mathbf{J}_N(k)$ is as given in (3.17) but with a modified scalar $d(k) \to d_N(k)$, i.e.,

$$\mathbf{J}_N(k) = \begin{pmatrix} 0 & d_N(k)(1 + i\delta k) \\ d_N^{-1}(k)(1 - i\delta k) & 0 \end{pmatrix}. \tag{3.51}$$

We follow the procedure outlined in articles [21, 10, 23, 22] closely and so do not give the arguments here, contained in those papers, for the convergence of approximate factors to the exact ones. It will suffice to later verify the results obtained herein by numerical experiment. The scalar $d_N(k)$ is any function which approximates $d(k)$ accurately in the strip $\mathcal{D}$, and for efficacy of the following method it is most convenient to use a rational function approximation

$$d_N(k) = \frac{P_N(k)}{Q_N(k)}, \tag{3.52}$$

where $P_N(k)$, $Q_N(k)$ are polynomial functions of order $N$. Note that the order of each polynomial is the same, as we require that $d_N(k) \to 1$ as $|k| \to \infty$. There is a variety of ways of generating the coefficients of these polynomials, and the simplest and perhaps most justifiable (in terms of its analyticity properties) is to use Padé approximants [28]. As a note of caution, we must check that $d_N(k)$ does not introduce spurious singularities into the strip of analyticity $\mathcal{D}$; otherwise we will produce an inaccurate factorization. One-point Padé approximants, if they exist, are determined uniquely from the Taylor series expansion of the original function at any point of regularity. If we work with the origin, then the (one-point) Padé approximant of $d(k)$ is found by solving

$$\sum_{i=0}^{\infty} e_i k^i - \frac{P_N(k)}{Q_N(k)} = \mathcal{O}(k^{2N+1}), \tag{3.53}$$

where $\sum_{i=0}^{\infty} e_i k^i$ is the Maclaurin expansion of $d(k)$. This provides ample accuracy for our purposes (see section 5), due to the rapid decay at large real $k$ that is otherwise present in the Fourier transform inversion formulas (4.7) and (4.8).

Note that the approximation of just $d(k)$ ensures that the scalar Khrapkov factors (3.35), (3.37) remain the same, etc., and so a partial decomposition of $\mathbf{K}_N(k)$ is simply

$$\mathbf{K}_N(k) = \mathbf{Q}_N^-(k)\mathbf{Q}_N^+(k), \tag{3.54}$$

in which $\mathbf{Q}_N^{\pm}(k)$ are given by (3.47), (3.48), with $\mathbf{R}^{\pm}(k)$ replaced by $\mathbf{R}_N^{\pm}(k)$ and $\mathbf{T}^{\pm}(k)$ replaced by $\mathbf{T}_N^{\pm}(k)$, for which the subscript $N$ denotes that $\mathbf{J}_N(k)$, given by (3.51), replaces $\mathbf{J}(k)$ everywhere. Thus, the factorization of $\mathbf{K}_N(k)$ has been accomplished apart from sequences of poles, arising from the zeros and poles of $d_N(k)$ occurring in both half-planes exterior to $\mathcal{D}$. If we can remove these singularities, then an explicit exact factorization of $\mathbf{K}_N(k)$ will have been achieved, which approximates the actual factors $\mathbf{K}^{\pm}(k)$ in their regions of analyticity.

**3.4.2. Removal of pole singularities.** The exact factorization of $\mathbf{K}_N(k)$, given by (3.49), may be written as

$$\mathbf{K}_N(k) = \mathbf{K}_N^-(k)\mathbf{K}_N^+(k), \tag{3.55}$$

$$\mathbf{K}_N^-(k) = \mathbf{Q}_N^-(k)\mathbf{M}(k), \qquad \mathbf{K}_N^+(k) = \mathbf{M}^{-1}(k)\mathbf{Q}_N^+(k), \tag{3.56}$$

in which $\mathbf{M}(k)$ must be a meromorphic matrix which has to be chosen to eliminate the poles of $\mathbf{Q}_N^-(k)$ in the lower half-plane and the poles of $\mathbf{Q}_N^+(k)$ in $\mathcal{D}^+$. We can pose a (nonunique) ansatz for $\mathbf{M}(k)$ after noting certain symmetry properties of $\mathbf{Q}_N^{\pm}(k)$. First, from (3.18),

$$d(-k) = 1/d(k), \tag{3.57}$$

which must be reflected in the similar approximant behavior:

$$d_N(-k) = 1/d_N(k). \tag{3.58}$$

Thus,

$$\mathbf{J}_N(-k) = [\mathbf{J}_N(k)]^T, \tag{3.59}$$

where the superscript denotes the transpose, and so by inspection of (3.45),

$$\mathbf{R}_N^+(-k) = [\mathbf{R}_N^-(k)]^T. \tag{3.60}$$

Similarly, from (3.36), (3.39) and the obvious evenness of $\Delta(k)$ in (3.20), changing $k$ to $-k$ in (3.29) reveals

$$\mathbf{T}_N^+(-k) = [\mathbf{T}_N^-(k)]^T. \tag{3.61}$$

Hence we find (see (3.48)) that

$$\mathbf{Q}_N^+(-k) = [\mathbf{T}_N^-(k)]^T[\mathbf{R}_N^-(k)]^T \begin{pmatrix} -ik & -ik \\ 1 & -1 \end{pmatrix}^T = [\mathbf{Q}_N^-(k)]^T \tag{3.62}$$

and deduce that the second equation in (3.56) gives

$$\mathbf{K}_N^+(-k) = \mathbf{M}^{-1}(-k)[\mathbf{Q}_N^-(k)]^T. \tag{3.63}$$

Symmetry properties dictate, by comparison with the first equation of (3.56), that we can construct a suitably scaled $\mathbf{M}(k)$ so that

$$\mathbf{M}^{-1}(-k) = [\mathbf{M}(k)]^T. \tag{3.64}$$

After this is achieved, it suffices to eliminate poles of $\mathbf{K}_N^-(k)$ in the lower half-plane.

Now suppose that $d_N(k)$ has $N_p$ poles in the upper half-plane at $k = ip_n$, $n = 1, 2, \ldots, N_p$ ($ip_n \notin \mathcal{D}^-$), and $N_q$ poles in the region below the strip at $k = -iq_n$, $n = 1, 2, \ldots, N_q$. That is, $Q_N(k)$ in (3.52) has zeros at $k = ip_n, -iq_n$. As has already been stated, there are, in total,

$$N_p + N_q = N \tag{3.65}$$

simple poles in the complex plane, and, due to the symmetry (3.58), there are $N$ simple zeros of $P_N(k)$ at

$$k = -ip_n, \qquad n = 1, 2 \ldots, N_p; \qquad k = iq_n, \qquad n = 1, 2 \ldots, N_q, \tag{3.66}$$

in the lower and upper regions, respectively. Thus, $d_N(k)$ and its inverse may be expressed as Mittag–Leffler expansions:

$$d_N(k) = 1 + \sum_{n=1}^{N_p} \frac{\alpha_n}{p_n + ik} + \sum_{n=1}^{N_q} \frac{\beta_n}{q_n - ik}, \tag{3.67}$$

$$\frac{1}{d_N(k)} = 1 + \sum_{n=1}^{N_p} \frac{\alpha_n}{p_n - ik} + \sum_{n=1}^{N_q} \frac{\beta_n}{q_n + ik}, \tag{3.68}$$

where both tend to unity at infinity by virtue of $d_N(k)$ being a one-point Padé approximant of $d(k)$ in (3.18). The coefficients $\alpha_n$, $\beta_n$ are easily determined from the coefficients of the polynomials $P_N(k)$, $Q_N(k)$, the numerator and denominator, respectively, of $d_N(k)$. By inspection of the location of $d_N(k)$ in $\mathbf{Q}_N^-(k)$, the ansatz for $\mathbf{M}(k)$ is now posed (cf. those offered in [10, 23]) as

$$\mathbf{M}(k) = \begin{pmatrix} \frac{1}{\sqrt{2}} + \sum_{n=1}^{N_p} \frac{A_n}{p_n + ik} + \sum_{n=1}^{N_q} \frac{B_n}{q_n - ik} & -\left( \frac{1}{\sqrt{2}} + \sum_{n=1}^{N_p} \frac{C_n}{p_n + ik} + \sum_{n=1}^{N_q} \frac{D_n}{q_n - ik} \right) \\ \left( \frac{1}{\sqrt{2}} + \sum_{n=1}^{N_p} \frac{C_n}{p_n - ik} + \sum_{n=1}^{N_q} \frac{D_n}{q_n + ik} \right) & \frac{1}{\sqrt{2}} + \sum_{n=1}^{N_p} \frac{A_n}{p_n - ik} + \sum_{n=1}^{N_q} \frac{B_n}{q_n + ik} \end{pmatrix}, \tag{3.69}$$

where $A_n$, $B_n$, $C_n$, $D_n$ are as yet undetermined constants. This form encapsulates the zeros and singularities of $d_N(k)$ and is chosen to satisfy the symmetry relation (3.64). However, the latter holds only if $|\mathbf{M}(k)| \equiv 1$, whereas (3.69) gives

$$\begin{aligned} |\mathbf{M}(k)| = &\left( \frac{1}{\sqrt{2}} + \sum_{n=1}^{N_p} \frac{A_n}{p_n + ik} + \sum_{n=1}^{N_q} \frac{\bar{B}_n}{q_n - ik} \right) \left( \frac{1}{\sqrt{2}} + \sum_{n=1}^{N_p} \frac{A_n}{p_n - ik} + \sum_{n=1}^{N_q} \frac{B_n}{q_n + ik} \right) \\ &+ \left( \frac{1}{\sqrt{2}} + \sum_{n=1}^{N_p} \frac{C_n}{p_n - ik} + \sum_{n=1}^{N_q} \frac{D_n}{q_n + ik} \right) \left( \frac{1}{\sqrt{2}} + \sum_{n=1}^{N_p} \frac{C_n}{p_n + ik} + \sum_{n=1}^{N_q} \frac{D_n}{q_n - ik} \right). \end{aligned} \tag{3.70}$$

The four sets of poles can be eliminated by setting the coefficients to satisfy the two

systems of equations

$$A_m\left(\frac{1}{\sqrt{2}}+\sum_{n=1}^{N_p}\frac{A_n}{p_n+p_m}+\sum_{n=1}^{N_q}\frac{B_n}{q_n-p_m}\right)$$
$$+C_m\left(\frac{1}{\sqrt{2}}+\sum_{n=1}^{N_p}\frac{C_n}{p_n+p_m}+\sum_{n=1}^{N_q}\frac{D_n}{q_n-p_m}\right)=0\quad(1\le m\le N_p), \tag{3.71}$$

$$B_m\left(\frac{1}{\sqrt{2}}+\sum_{n=1}^{N_p}\frac{A_n}{p_n-q_m}+\sum_{n=1}^{N_q}\frac{B_n}{q_n+q_m}\right)$$
$$+D_m\left(\frac{1}{\sqrt{2}}+\sum_{n=1}^{N_p}\frac{C_n}{p_n-q_m}+\sum_{n=1}^{N_q}\frac{D_n}{q_n+q_m}\right)=0\quad(1\le m\le N_q). \tag{3.72}$$

Then $|\mathbf{M}(k)|$ is entire and takes the value unity at infinity. Hence Liouville's theorem implies that the determinant is indeed $|\mathbf{M}(k)|=1$ everywhere, as required.

By premultiplying $\mathbf{M}(k)$ by $\mathbf{R}^-(k)\mathbf{T}^-(k)$ and eliminating poles in the lower half-plane, conditions relating these coefficients can be found. From (3.29) and (3.45) we know that

$$\left[(1+ik\beta^2\gamma)\mathbf{I}+\mathbf{J}_N(k)\right]$$
$$\times\left[\cosh[\Delta(k)\theta^-(k)]\mathbf{I}+\frac{1}{\Delta(k)}\sinh[\Delta(k)\theta^-(k)]\mathbf{J}_N(k)\right]\mathbf{M}(k) \tag{3.73}$$

must be analytic in $\mathcal{D}^-$, and so from (3.51) we wish to remove poles in the lower half-plane from

$$\begin{pmatrix} a^-(k) & b^-(k)(1+i\delta k)d_N(k) \\ b^-(k)(1-i\delta k)/d_N(k) & a^-(k)\end{pmatrix}\mathbf{M}(k), \tag{3.74}$$

where

$$a^\pm(k)=(1\mp ik\beta^2\gamma)\cosh[\Delta(k)\theta^\pm(k)]+\Delta(k)\sinh[\Delta(k)\theta^\pm(k)], \tag{3.75}$$

$$b^\pm(k)=\cosh[\Delta(k)\theta^\pm(k)]+\frac{(1\mp ik\beta^2\gamma)}{\Delta(k)}\sinh[\Delta(k)\theta^\pm(k)] \tag{3.76}$$

are scalar functions analytic in the indicated regions. Note that

$$a^-(k)=a^+(-k),\qquad b^-(k)=b^+(-k). \tag{3.77}$$

The top-left element of the matrix in (3.74) is, by employing (3.67),

$$a^-(k)\left(\frac{1}{\sqrt{2}}+\sum_{n=1}^{N_p}\frac{A_n}{p_n+ik}+\sum_{n=1}^{N_q}\frac{B_n}{q_n-ik}\right)+b^-(k)(1+i\delta k)$$
$$\times\left(1+\sum_{n=1}^{N_p}\frac{\alpha_n}{p_n+ik}+\sum_{n=1}^{N_q}\frac{\beta_n}{q_n-ik}\right)\left(\frac{1}{\sqrt{2}}+\sum_{n=1}^{N_p}\frac{C_n}{p_n-ik}+\sum_{n=1}^{N_q}\frac{D_n}{q_n+ik}\right), \tag{3.78}$$

which appears to contain simple poles at $k=-ip_n$, $n=1,\dots,N_p$, $k=-iq_n$, $n=1,\dots,N_q$, in the lower half-plane unless they are suppressed. However, there are in

fact no poles at $k = -ip_n$ because the sum of these terms multiplies $d_N(k)$, which we know is zero at these points. Thus, setting the expression in (3.78) to remain finite at the remaining singularity locations $k = -iq_n$ gives the relation, after use of (3.77),

(3.79)
$$a^+(iq_m)B_m + b^+(iq_m)\beta_m(1+\delta q_m)\left(\frac{1}{\sqrt{2}} + \sum_{n=1}^{N_p}\frac{C_n}{p_n - q_m} + \sum_{n=1}^{N_q}\frac{D_n}{q_n + q_m}\right) = 0, \quad 1 \le m \le N_q.$$

Similarly the bottom-left element of (3.74) contains no poles in the lower half-plane if and only if

(3.80)
$$a^+(ip_m)C_m + b^+(ip_m)\alpha_m(1-\delta p_m)\left(\frac{1}{\sqrt{2}} + \sum_{n=1}^{N_p}\frac{A_n}{p_n + p_m} + \sum_{n=1}^{N_q}\frac{B_n}{q_n - p_m}\right) = 0, \quad 1 \le m \le N_p.$$

Likewise, suppression of the lower half-plane poles in the second column of (3.74) yields

(3.81)
$$a^+(iq_m)D_m - b^+(iq_m)\beta_m(1+\delta q_m)\left(\frac{1}{\sqrt{2}} + \sum_{n=1}^{N_p}\frac{A_n}{p_n - q_m} + \sum_{n=1}^{N_q}\frac{B_n}{q_n + q_m}\right) = 0, \quad 1 \le m \le N_q,$$

(3.82)
$$a^+(ip_m)A_m - b^+(ip_m)\alpha_m(1-\delta p_m)\left(\frac{1}{\sqrt{2}} + \sum_{n=1}^{N_p}\frac{C_n}{p_n + p_m} + \sum_{n=1}^{N_q}\frac{D_n}{q_n - p_m}\right) = 0, \quad 1 \le m \le N_p.$$

By inspection, (3.79), (3.81) imply (3.72) and similarly (3.80), (3.82) imply (3.71). Therefore, not only do (3.79)–(3.82) enforce $\mathbf{K}_N^-(k)$ to be analytic in $\mathcal{D}^-$ as required, but relations (3.56), (3.62)–(3.64) reveal that they are also sufficient to ensure that $\mathbf{K}_N^+(k)$ is free of singularities in the half-plane $\mathcal{D}^+$, as are the inverses $[\mathbf{K}_N^\pm(k)]^{-1}$ in their indicated half-planes $\mathcal{D}^\pm$.

Thus (3.79)–(3.82) constitute a linear system of $2N$ equations for the $2N$ unknowns $A_m$, $B_m$, $C_n$, $D_n$ and are easily solved to determine their values. Note that it may transpire that $1+\delta q_m$ or $1-\delta p_m$ is zero for particular choices of $m$, $h$, $N$, etc., in which case $(B_m, D_m)$ or $(A_m, C_m)$ would vanish. However, this does not present any difficulty (cf. equation (80) in [10]), and no cases have been encountered in which the system for $A_m$–$D_m$ is singular.

**3.4.3. Approximate noncommutative factorization.** The explicit approximate factorization of $\mathbf{K}(k)$ is complete, having obtained an exact noncommutative matrix product decomposition of $\mathbf{K}_N(k)$. The factors $\mathbf{K}_N^\pm(k)$ are constructed from

(3.56), with $\mathbf{Q}_N^{\pm}(k)$ given from (3.51), (3.47), (3.48), (3.45), and (3.29). The meromorphic matrix $\mathbf{M}(k)$ takes the explicit form (3.69), in which the coefficients satisfy algebraic equations (3.79)–(3.82). As $N$ increases it is expected that $\mathbf{K}_N^{\pm}(k)$ will converge rapidly to the exact factors $\mathbf{K}^{\pm}(k)$, and this will be borne out by numerical results given in section 5. All that remains here is to verify that the apparent pole at $k = 0$ in $\mathbf{R}^{\pm}(k)$ is removed and to give the behavior of $\mathbf{K}_N^{\pm}(k)$ for large $|k|$ in $\mathcal{D}^{\pm}$.

As $k \to 0$, we know that $d_N(k) \to 1$ by virtue of the function $d(k)$ in (3.18), and hence $\mathbf{R}_N^{\pm}(k)$ behaves as, from (3.45), (3.51),

$$\mathbf{R}_N^{\pm}(k) = \frac{\mp i}{2\beta^2 k\gamma} \begin{pmatrix} 1 & 1 \\ 1 & 1 \end{pmatrix} + \mathcal{O}(1). \tag{3.83}$$

Therefore,

$$\begin{pmatrix} -ik & -ik \\ 1 & -1 \end{pmatrix} \mathbf{R}_N^{-}(k) \sim \frac{1}{\beta^2\gamma} \begin{pmatrix} 1 & 1 \\ 0 & 0 \end{pmatrix} + \mathcal{O}(1), \qquad k \to 0. \tag{3.84}$$

Now, $\mathbf{T}_N^{\pm}(k)$, from their definitions, are bounded at the origin, and, by inspection, so is $\mathbf{M}(k)$ in (3.69). Hence, from (3.56) and (3.84) we can deduce that

$$\mathbf{K}_N^{-}(k) = \mathcal{O}(1), \qquad k \to 0. \tag{3.85}$$

Similarly, from above,

$$\mathbf{R}_N^{+}(k) \begin{pmatrix} ik & 1 \\ ik & -1 \end{pmatrix} = \mathcal{O}(1), \qquad k \to 0, \tag{3.86}$$

and so $\mathbf{K}_N^{+}(0)$ is bounded too.

As $|k|$ tends to infinity it is a straightforward matter to deduce the asymptotic behavior of the product factors. First, by inspection of (3.45),

$$\mathbf{R}_N^{\pm}(k) \sim \frac{i}{2\beta^2 k} \begin{pmatrix} \mp\beta^2\gamma & +\delta \\ -\delta & \mp\beta^2\gamma \end{pmatrix}, \tag{3.87}$$

in view of the fact that we *defined* $d_N(k)$ in $\mathbf{J}_N(k)$ to behave as

$$d_N(k) \to 1, \qquad |k| \to \infty. \tag{3.88}$$

Second, the asymptotic form of the Krapkhov decomposition elements $r^{\pm}(k)$, $\theta^{\pm}(k)$ can be deduced from their integral definitions written in (3.37), (3.39), and (3.35), (3.36), respectively. The latter identities are easily shown to give

$$\theta^{\pm}(k) = \pm\epsilon/k + \mathcal{O}(k^{-2}), \qquad |k| \to \infty, k \in \mathcal{D}^{\pm}, \tag{3.89}$$

where

$$\epsilon = \frac{i}{\pi} \int_0^{\infty} \frac{1}{\Delta(\zeta)} \tanh^{-1} \left\{ \frac{\sqrt{f^2(\zeta) + e^2(\zeta)}(1 + \beta^2\zeta^2) - \Delta(\zeta)g(\zeta)}{g(\zeta)(1 + \beta^2\zeta^2) - \Delta(\zeta)\sqrt{f^2(\zeta) + e^2(\zeta)}} \right\} d\zeta, \tag{3.90}$$

and for $r^{\pm}(k)$ the integral in the exponent of (3.37) is also $\mathcal{O}(k^{-1})$ for large $|k|$. Hence by inspection we find that

$$r^{\pm}(k) = 2\beta(\mp ik)^{3/2} + \mathcal{O}(k^{1/2}), \qquad |k| \to \infty, k \in \mathcal{D}^{\pm}, \tag{3.91}$$

and so the asymptotic form of $\mathbf{T}_N^{\pm}(k)$, (3.29), is

$$\mathbf{T}_N^{\pm}(k) \sim 2\beta(\mp ik)^{3/2} \begin{pmatrix} \cosh(\epsilon\delta) & \pm i\sinh(\epsilon\delta) \\ \mp i\sinh(\epsilon\delta) & \cosh(\epsilon\delta) \end{pmatrix}. \tag{3.92}$$

Therefore, $\mathbf{Q}_N^{\pm}(k)$ in (3.47), (3.48) can be estimated. Finally, the meromorphic matrix (3.69) has the large $|k|$ form

$$\mathbf{M}(k) = \frac{1}{\sqrt{2}} \begin{pmatrix} 1 & -1 \\ 1 & 1 \end{pmatrix}. \tag{3.93}$$

Thus the asymptotic growth of $\mathbf{K}_N^{\pm}(k)$ in (3.56) is found to be

$$\begin{aligned} \mathbf{K}_N^{-}(k) \sim & -\frac{(ik)^{1/2}}{\sqrt{2}\beta} \begin{pmatrix} -ik & -ik \\ 1 & -1 \end{pmatrix} \begin{pmatrix} \beta^2\gamma & \delta \\ -\delta & \beta^2\gamma \end{pmatrix} \\ & \times \begin{pmatrix} \cosh(\epsilon\delta) & -i\sinh(\epsilon\delta) \\ +i\sinh(\epsilon\delta) & \cosh(\epsilon\delta) \end{pmatrix} \begin{pmatrix} 1 & -1 \\ 1 & 1 \end{pmatrix}, \end{aligned} \tag{3.94}$$

$$\begin{aligned} \mathbf{K}_N^{+}(k) \sim & -\frac{(-ik)^{1/2}}{\sqrt{2}\beta} \begin{pmatrix} 1 & 1 \\ -1 & 1 \end{pmatrix} \begin{pmatrix} \cosh(\epsilon\delta) & i\sinh(\epsilon\delta) \\ -i\sinh(\epsilon\delta) & \cosh(\epsilon\delta) \end{pmatrix} \\ & \times \begin{pmatrix} \beta^2\gamma & -\delta \\ \delta & \beta^2\gamma \end{pmatrix} \begin{pmatrix} ik & 1 \\ ik & -1 \end{pmatrix}. \end{aligned} \tag{3.95}$$

The kernel decomposition is now complete.

**4. Solution of the Wiener–Hopf equation.** Having obtained an approximate factorization of $\mathbf{K}(k)$, it is now a straightforward matter to complete the solution of the Wiener–Hopf equation (2.18). Dropping the subscript $N$ in the factorization (3.55) for brevity, the Wiener–Hopf equation can be recast into the form

$$\begin{aligned} & [\mathbf{K}^-(k)]^{-1} \begin{pmatrix} T^-(k) \\ -S^-(k) \end{pmatrix} - \frac{i}{k+i\epsilon} \left\{ [\mathbf{K}^-(k)]^{-1} - [\mathbf{K}^-(-i\epsilon)]^{-1} \right\} \\ & \times \left( U \frac{h+1}{h} \begin{bmatrix} 0 \\ 1 \end{bmatrix} + \frac{1}{2\mu} \begin{bmatrix} 2G_+ - 2G_- \\ G_+h + G_- \end{bmatrix} \right) = \mathbf{E}(k) = \mathbf{K}^+(k) \begin{pmatrix} \Psi^+(k,0) \\ \Psi_y^+(k,0) \end{pmatrix} \\ & + \frac{i}{k+i\epsilon} [\mathbf{K}^-(-i\epsilon)]^{-1} \left( U \frac{h+1}{h} \begin{bmatrix} 0 \\ 1 \end{bmatrix} + \frac{1}{2\mu} \begin{bmatrix} 2G_+ - 2G_- \\ G_+h + G_- \end{bmatrix} \right), \end{aligned} \tag{4.1}$$

where $k \in \mathcal{D}$. The left-hand side is analytic in $\mathcal{D}^-$, whereas the right-hand side is regular in $\mathcal{D}^+$. Thus the equation has been arranged so that the two sides offer analytic continuation into the whole complex $k$-plane which must therefore be equal to an entire function, denoted $\mathbf{E}(k)$, say. To determine $\mathbf{E}(k)$ we must examine the growth at infinity of both sides of (4.1) in their respective half-planes of analyticity. To do this we require the large $k$ behavior of $T^-(k)$, $S^-(k)$, $\Psi^+(k)$, $\Psi_y^+(k)$, which relate directly to the values of the untransformed physical variables near the tip of the splitter plate. For example, a function which behaves like $x^n$, $x \to 0+$, has a half-range (0 to $\infty$) Fourier transform which decays like $\mathcal{O}(k^{-n-1})$, $k \to \infty$, in the

upper half-plane (see equation (1.74) of [1]). Hence from (2.27) and (2.29) we deduce, respectively, that

$$\Psi^+(k,0) = \mathcal{O}(k^{-5/2}), \qquad \Psi^+_y(k,0) = \mathcal{O}(k^{-3/2}) \tag{4.2}$$

as $|k| \to \infty$, $k \in \mathcal{D}^+$ and hence

$$\begin{pmatrix} T^-(k) \\ -S^-(k) \end{pmatrix} - \frac{i}{k}\left(U\frac{h+1}{h}\begin{bmatrix} 0 \\ 1 \end{bmatrix} + \frac{1}{2\mu}\begin{bmatrix} 2G_+ - 2G_- \\ G_+h + G_- \end{bmatrix}\right) = \begin{pmatrix} \mathcal{O}(k^{1/2}) \\ \mathcal{O}(k^{-1/2}) \end{pmatrix} \tag{4.3}$$

as $|k| \to \infty, k \in \mathcal{D}^-$. These are used, together with the asymptotic forms (3.94), (3.95), to reveal that both elements of the left-hand side of (4.1) decay as $\mathcal{O}(k^{-1})$ in the lower half-plane, and similarly the right-hand side has the form $\mathcal{O}(k^{-1})$ as $|k| \to \infty$ in the upper half-plane. Hence, $\mathbf{E}(k)$ is an entire function which decays to zero at infinity and so, by Liouville's theorem, is identically zero. Thus, the solution of the Wiener–Hopf equation is

$$\begin{pmatrix} \Psi^+(k,0) \\ \Psi^+_y(k,0) \end{pmatrix} = -\frac{i}{k+i\epsilon}[\mathbf{K}^+(k)]^{-1}[\mathbf{K}^-(-i\epsilon)]^{-1} \times \left(U\frac{h+1}{h}\begin{bmatrix} 0 \\ 1 \end{bmatrix} + \frac{1}{2\mu}\begin{bmatrix} 2G_+ - 2G_- \\ G_+h + G_- \end{bmatrix}\right) \tag{4.4}$$

or, equivalently,

$$\begin{pmatrix} T^-(k) \\ -S^-(k) \end{pmatrix} = \frac{i}{k+i\epsilon}\left\{\mathbf{I} - \mathbf{K}^-(k)[\mathbf{K}^-(-i\epsilon)]^{-1}\right\} \times \left(U\frac{h+1}{h}\begin{bmatrix} 0 \\ 1 \end{bmatrix} + \frac{1}{2\mu}\begin{bmatrix} 2G_+ - 2G_- \\ G_+h + G_- \end{bmatrix}\right). \tag{4.5}$$

From this we can directly deduce the coefficients $A(k)$–$D(k)$, via (2.16), (2.17), and hence establish $\Psi(k,y)$ in $-1 < y < h$, from (2.14), (2.15). Finally, on setting the convergence factor $\epsilon$ to zero in (4.4), the disturbance stream function is

$$\bar{\psi} = \frac{1}{2\pi}\int_{-\infty}^{\infty} \Psi(k,y)e^{-ikx}dk, \tag{4.6}$$

where the integral path runs along the real line indented above the origin, and

$$\Psi(k,y) = \frac{-i}{\sinh^2 k - k^2}\begin{pmatrix} (1+y)\sinh[k(1+y)] \\ (1+y)\cosh[k(1+y)] - k^{-1}\sinh[k(1+y)] \end{pmatrix}^T \times \begin{pmatrix} k\sinh k & -(\cosh k - k^{-1}\sinh k) \\ -(k\cosh k + \sinh k) & \sinh k \end{pmatrix}[\mathbf{K}^+(k)]^{-1}[\mathbf{K}^-(0)]^{-1} \times \left(U\frac{h+1}{h}\begin{bmatrix} 0 \\ 1 \end{bmatrix} + \frac{1}{2\mu}\begin{bmatrix} 2G_+ - 2G_- \\ G_+h + G_- \end{bmatrix}\right) \tag{4.7}$$

in $-1 < y < 0$, whereas in $0 < y < h$

$$\Psi(k,y) = \frac{-i}{\sinh^2 kh - k^2h^2}\begin{pmatrix} (h-y)\sinh[k(h-y)] \\ (h-y)\cosh[k(h-y)] - k^{-1}\sinh[k(h-y)] \end{pmatrix}^T \times \begin{pmatrix} kh\sinh kh & h\cosh kh - k^{-1}\sinh kh \\ -(kh\cosh kh + \sinh kh) & -h\sinh kh \end{pmatrix}[\mathbf{K}^+(k)]^{-1}[\mathbf{K}^-(0)]^{-1} \times \left(U\frac{h+1}{h}\begin{bmatrix} 0 \\ 1 \end{bmatrix} + \frac{1}{2\mu}\begin{bmatrix} 2G_+ - 2G_- \\ G_+h + G_- \end{bmatrix}\right). \tag{4.8}$$

It is a straightforward matter to verify that this solution satisfies the biharmonic equation and the boundary and jump conditions (2.4), (2.5), (2.7). From this the downstream velocity field is determined from (2.3).

Formulas (4.7), (4.8) are suitable for evaluating $\bar{\psi}$, given by (4.6), in the $x < 0$ channels by completing the contour in the upper half-plane. Consistent with (2.3), there is no contribution from the pole at $k = 0$ to (4.6), which consists of Papkovich–Fadle strip eigenfunctions, generated by residues at the zeros of $\sinh^2 k - k^2$ or $\sinh^2 kh - k^2h^2$. These infinite sums describe how, in each channel, the flow differs from its far downstream profile $u^\infty_\pm$.

However, the evaluation of $\bar{\psi}$ in the upstream ($x > 0$) channel is achieved by completing the contour in the lower half-plane. When $[\mathbf{K}^+(k)]^{-1}$ is replaced, according to (3.1), by $\operatorname{adj}\mathbf{K}(k)\mathbf{K}^-(k)/|\mathbf{K}(k)|$, the substitution of (2.19), (2.24) into (4.7) yields

$$\Psi(k,y) \tag{4.9}$$

$$= \frac{i}{k^2[\sinh^2 k(h+1) - k^2(h+1)^2]} \begin{pmatrix} (1+y)\sinh[k(1+y)] \\ (1+y)\cosh[k(1+y)] - k^{-1}\sinh[k(1+y)] \end{pmatrix}^T$$

$$\times \mathbf{V}(k) \begin{pmatrix} 1 & 0 \\ 0 & -k \end{pmatrix} \mathbf{K}^-(k)[\mathbf{K}^-(0)]^{-1} \left( U\frac{h+1}{h} \begin{bmatrix} 0 \\ 1 \end{bmatrix} + \frac{1}{2\mu} \begin{bmatrix} 2G_+ - 2G_- \\ G_+h + G_- \end{bmatrix} \right),$$

in which the elements of $\mathbf{V}(k)$ are concisely defined by

$$V_{11} + V_{22} = kh(h+1)\sinh k, \qquad V_{11} - V_{22} = -\sinh kh \sinh k(h+1),$$

$$V_{21} + V_{12} = k^{-1}\sinh kh \sinh k(h+1) - kh(h+1)\cosh k,$$

$$V_{21} - V_{12} = \sinh kh \cosh k(h+1) - h\sinh k.$$

The residue at the pole $k = 0$ yields the upstream behavior ($x \to \infty$)

$$\bar{\psi} \sim h \begin{pmatrix} \left(\frac{1+y}{h+1}\right)^2 & \left(\frac{1+y}{h+1}\right)^3 \end{pmatrix} \begin{pmatrix} -\frac{h}{2} & 1 - \frac{h}{2} \\ \frac{h}{6}(h+3) & -1 \end{pmatrix} \tag{4.10}$$

$$\times \left( U\frac{h+1}{h} \begin{bmatrix} 0 \\ 1 \end{bmatrix} + \frac{1}{2\mu} \begin{bmatrix} 2G_+ - 2G_- \\ G_+h + G_- \end{bmatrix} \right)$$

in $-1 < y < 0$, which, when substituted into (2.3), gives the net upstream flow form. That is, the $y$-derivative of (4.10) is verified, with use of (1.5), to equal $u^\infty(y) - u^\infty_-(y)$, given by (1.1), (1.3). A similar calculation, based on (4.8), verifies that $u^\infty(y) - u^\infty_+(y)$ is obtained in $(0, h)$. Identical series of Papkovich–Fadle eigenfunctions arise in (4.6) from residues associated with the zeros of $[\sinh^2 k(h+1) - k^2(h+1)^2]$. This infinite sum describes how the flow differs from its far upstream profile $u^\infty$ in $-1 < y < h$.

**5. Numerical computation.** The calculations are performed with MATLAB, except for the evaluation of the Padé approximants $d_{2m}$ by means of Maple. The resulting fractions are then converted to floating points (16 digit accuracy) and returned to MATLAB. Accuracy is low unless $N = 2M$ with $M$ even to take account of symmetries about both axes. Maximum accuracy occurs at about $N = 2$, $M = 16$ and could be increased by means of variable precision arithmetic. The poles $ip_m, -iq_m$

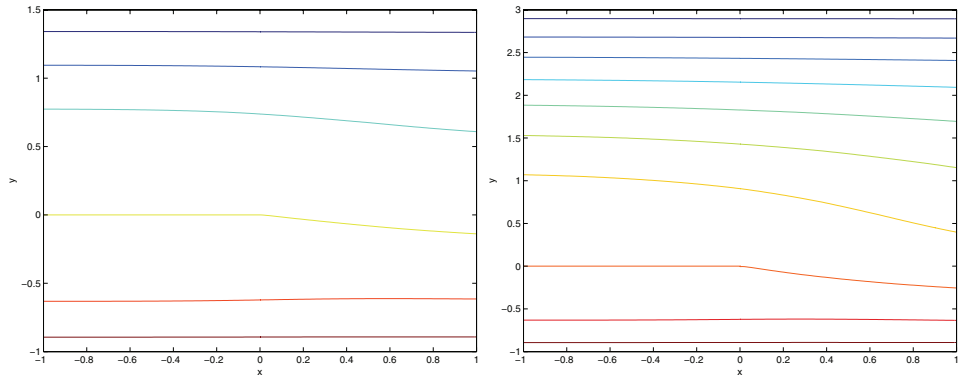


FIG. 5.1. *Stream function plots for the downstream shear case with* $U = 1$ *for (left)* $h = 1.5$ *and (right)* $h = 3$ *(note the different y-scale). The difference in stream function values (volume flux) between contours is* 0.2.

and coefficients $\alpha_m, \beta_m$ in (3.67) are then readily determined, followed by $\mathbf{J}_N(k)$ and $\mathbf{R}_N^+(k)$. Evaluation of $r_N^+(k), \theta_N^+(k)$ yields $\mathbf{T}_N^+(k)$ and hence $\mathbf{Q}_N^+(k)$, given by (3.48). The scalar Wiener–Hopf decomposition of $r$ and $\theta$ is achieved by using standard MATLAB numerical integration. The default relative accuracy of $10^{-6}$ easily suffices because higher accuracy is actually obtained, as in many contour integrals of analytic functions. Finally, $\mathbf{K}_N^+(k)$ is constructed. The stream function, $\psi(x, y)$, is evaluated in either of the $x < 0$ channels as a sum of the residues of (4.7) or (4.8) at the respective first 50 poles in the upper half-plane. Note that knowledge of the two sets of residues allows the inverse Fourier transform (4.6) to be computed for any $x(< 0)$ at essentially zero marginal cost. The companion matrix function $\mathbf{K}_N^-(k)$, needed in (4.9) for $x > 0$, is constructed similarly.

The numerical evaluation of the approximation $[\mathbf{K}_N^+(k)]^{-1}$ to $[\mathbf{K}^+(k)]^{-1}$ in (4.7), (4.8) depends on the accurate determination of the coefficients $a^+(ip_m), \ldots$ in (3.79)–(3.82). These are given by (3.75), (3.76), in which $\Delta(k)$ appears analytically, but branch cuts may arise from the presence $\theta^{\pm}(k)$ in the sinh functions. By factoring $\Delta(\zeta)$ from the numerator of the fraction in (3.35), it is evident that the branch cuts created by the approximate factorization arise solely from the square root in the definition (3.16) of $\mathbf{L}(k)$.

Very high accuracy would require variable precision arithmetic and a large number of terms in the residue sum, especially when computing the stream function values near the entrance to the downstream channels.

Figure 5.1 displays streamlines for $h = 1.5$ and $h = 3$ in the downstream shear case ($G_+ = 0 = G_-$). For the same values of $h$, Figure 5.2 shows streamlines when the walls are stationary ($U = 0$) with respective flux ratios $\Lambda = 1, -0.5, -2$, which typify the physically distinct ranges, $\Lambda > 0$, $-1 < \Lambda < 0$, $\Lambda < -1$. The curves have an imperceptible defect at $x = 0$; the values of $\psi(0, y)$ computed using (4.7) and (4.9) are not exactly the same in the Padé approximant technique but would be identical for the exact matrix $\mathbf{K}$. This discrepancy provides an estimate of the error, which is found to decrease with $N$ until at least $N = 12$, which is the value used in the figures. While the qualitative behavior in the pressure-driven case depends only on $\Lambda$, plots require a normalization of $G_-$ and $G_+$: for convenience, $G_- = 12\mu$ was taken.

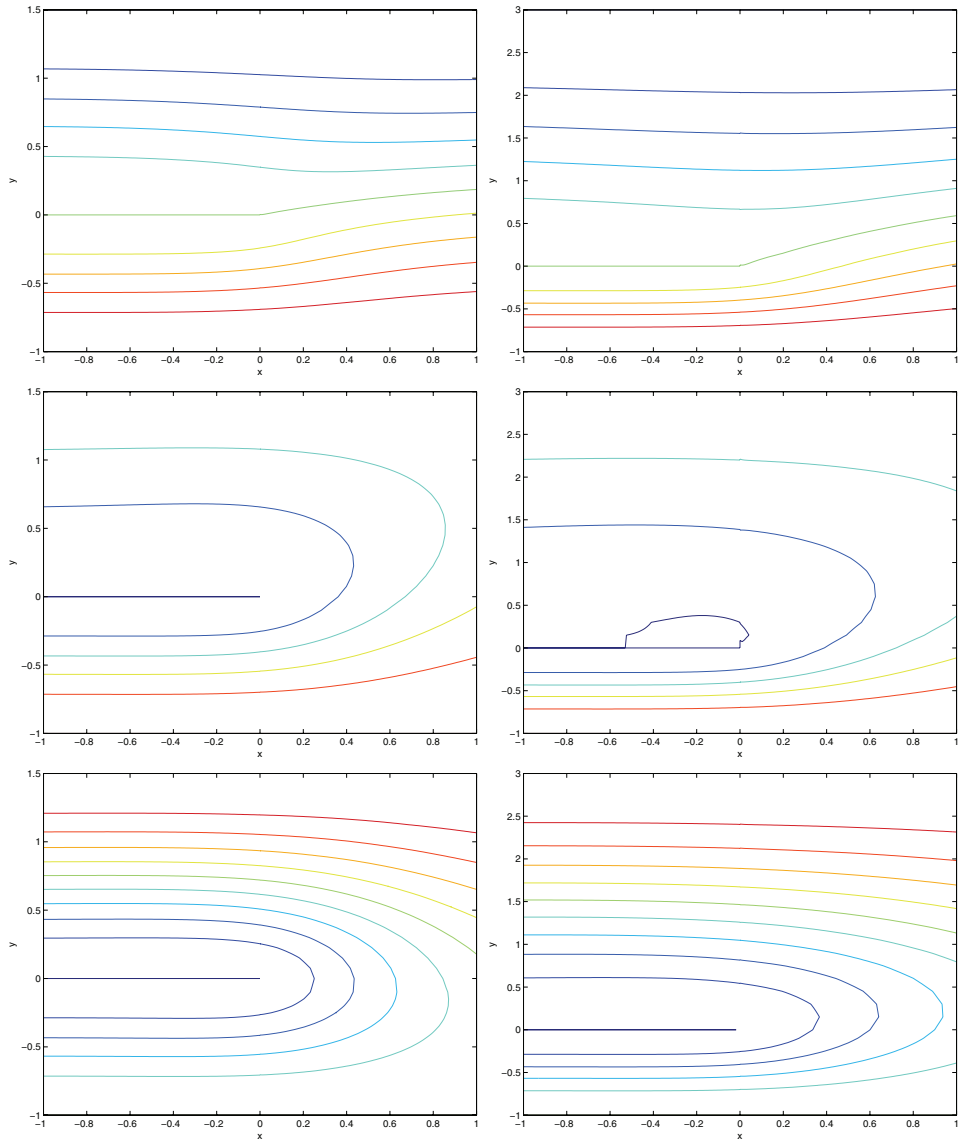

FIG. 5.2. *Stream function plots for the pressure-driven case. Left-hand panels:* $h = 1.5$*; right-hand panels:* $h = 3$*. Top row:* $\Lambda = 1$*, middle row:* $\Lambda = -0.5$*, bottom row:* $\Lambda = -2$*. The difference in stream function values (volume flux) between contours is* 0.2*. The jagged contour for* $h = 3$*,* $\Lambda = -0.5$ *is a contouring artifact.*

**6. Conclusion.** The Padé approximant technique for matrix Wiener–Hopf equations yields accurate numerical results for a classic Stokes flow problem for all channel width ratios. The theory is complicated by the need for successive modifications $\mathbf{L}$, $\mathbf{T}$ of the kernel and $\mathbf{M}$, $\mathbf{M}^{-1}$ of the matrix factors $\mathbf{Q}^-$, $\mathbf{Q}^+$ in order to establish the required analyticity of $\mathbf{K}^-$ and $\mathbf{K}^+$. The numerical implementation is not difficult conceptually but demands the usual careful attention to the analyticity properties of the functions involved. The technique provides a constructive scheme to obtain the physical solution without the major difficulties encountered in matching the three sets

of biorthogonal Papkovich–Fadle eigenfunctions.

## REFERENCES


[1] B. Noble, *Methods Based on the Wiener–Hopf Technique*, 2nd ed., Chelsea Press, New York, 1988.

[2] V. T. Buchwald and H. E. Doran, *Eigenfunctions of plane elastostatics. II. A mixed boundary value problem of the strip*, Proc. Roy. Soc. Ser. A, 284 (1965), pp. 69–82.

[3] R. M. L. Foote and V. T. Buchwald, *An exact solution for the stress intensity factor for a double cantilever beam*, Int. J. Fracture, 29 (1985), pp. 125–134.

[4] W. P. Graebel, *Slow viscous shear flow past a plate in a channel*, Phys. Fluids, 8 (1965), pp. 1929–1935.

[5] W. T. Koiter, *Approximate solution of Wiener–Hopf type integral equations with applications. I. General theory*, Proc. Acad. Sci. Amst. B, 57 (1954), pp. 558–579.

[6] S. Richardson, *A "stick-slip" problem related to the motion of a free jet at low Reynolds numbers*, Proc. Camb. Phil. Soc., 67 (1970), pp. 477–489.

[7] O. E. Jensen and D. Halpern, *The stress singularity in surfactant-driven thin-film flows. Part 1. Viscous effects*, J. Fluid Mech., 372 (1998) pp. 273–300.

[8] A. M. Moore, V. T. Buchwald, and M. E. Brewster, *The Stokesian entry flow*, Quart. J. Mech. Appl. Math., 43 (1990), pp. 107–133.

[9] M.-U. Kim, D. H. Choi, and J.-T. Jeong, *A two-dimensional model of a half-pitot tube*, Fluid Dyn. Res., 5 (1989), pp. 135–145.

[10] I. D. Abrahams, *On the solution of Wiener–Hopf problems involving noncommutative matrix kernel decompositions*, SIAM J. Appl. Math., 57 (1997), pp. 541–567.

[11] T. E. Stanton, D. Marshall, and C. N. Bryant, *On the conditions at the boundary of a fluid in turbulent motion*, Proc. Roy. Soc. Lond. A, 97 (1920), pp. 413–434.

[12] G. I. Taylor, *Measurements with a half-pitot tube*, Proc. Roy. Soc. Lond. A, 166 (1938), pp. 476–481.

[13] J. D. Fehribach and A. M. J. Davis, *Stokes flow around an asymmetric channel divider; a computational approach using MATLAB*, J. Engrg. Math., 39 (2001), pp. 207–220.

[14] H. Lamb, *Hydrodynamics*, 6th ed., Cambridge University Press, Cambridge, UK, 1993.

[15] W. D. Collins, *A note on the axisymmetric Stokes flow of viscous fluid past a spherical cap*, Mathematika, 10 (1963), pp. 72–79.

[16] A. M. J. Davis, *Axisymmetric Stokes flow past a spherical hollow boundary and concentric sphere*, Quart. J. Mech. Appl. Math., 38 (1985), pp. 537–559.

[17] I. C. Gohberg and M. G. Krein, *Systems of integral equations on a half-line with kernels depending on the difference of arguments*, Amer. Math. Soc. Transl. (2), 14 (1960), pp. 217–287.

[18] R. A. Hurd, *The Wiener–Hopf Hilbert method for diffraction problems*, Canad. J. Phys., 54 (1976), pp. 775–780.

[19] A. A. Khrapkov, *Certain cases of the elastic equilibrium of an infinite wedge with a nonsymmetric notch at the vertex, subjected to concentrated forces*, Appl. Math. Mech. (PMM), 35 (1971), pp. 625–637.

[20] V. G. Daniele, *On the factorization of Wiener–Hopf matrices in problems solvable with Hurd's method*, IEEE Trans. Antennas and Propagation, 26 (1978), pp. 614–616.

[21] I. D. Abrahams, *Radiation and scattering of waves on an elastic half-space; a noncommutative matrix Wiener–Hopf problem*, J. Mech. Phys. Solids, 44 (1996), pp. 2125–2154.

[22] I. D. Abrahams, *On the application of the Wiener–Hopf technique to problems in dynamic elasticity*, Wave Motion, 36 (2002), pp. 311–333.

[23] I. D. Abrahams, *On the non-commutative factorization of Wiener–Hopf kernels of Khrapkov type*, R. Soc. Lond. Proc. Ser. A Math. Phys. Eng. Sci., 454 (1998), pp. 1719–1743.

[24] M. Idemen, *A new method to obtain exact solutions of vector Wiener–Hopf equations*, Z. Angew. Math. Mech., 59 (1976), pp. 656–658.

[25] A. D. Rawlins, *Simultaneous Wiener–Hopf equations*, Canad. J. Phys., 58 (1980), pp. 420–428.

[26] I. D. Abrahams, *Scattering of sound by two parallel semi-infinite screens*, Wave Motion, 9 (1987), pp. 289–300.

[27] I. D. Abrahams and G. R. Wickham, *The scattering of water waves by two semi-infinite opposed vertical walls*, Wave Motion, 14 (1991), pp. 145–168.

[28] G. A. Baker, Jr., and P. Graves-Morris, *Padé Approximants*, 2nd ed., Cambridge University Press, Cambridge, UK, 1996.